PCCP

Accepted Manuscript

ROYAL SOCIETY OF CHEMISTRY

www.rsc.org/pccp

Solid State p-Type Dye-Sensitized Solar Cells: Concept, Experiment and Mechanism

Lei Zhang, Gerrit Boschloo, Leif Hammarström, Haining Tian*

Physical Chemistry, Department of Chemistry-Ångström Laboratory, Uppsala University, BOX 523, Uppsala SE 75120, Sweden. Email: haining.tian@kemi.uu.se

Abstract: Solid state p-type dye-sensitized solar cells (p-ssDSCs) have been proposed and fabricated for the first time, using an organic dye P1 as sensitizer on mesoporous NiO and phenyl-C61-butyric acid methyl ester (PCBM) as electron conductor. The p-ssDSC has shown an impressive open circuit photovoltage, 620 mV. Femtosecond and nanosecond transient absorption spectroscopy has given evidence for sub-ps hole injection from excited P1 to NiO, followed by electron transfer from $P1^{\bullet-}$ to PCBM.

Broader Context

Utilizing sun energy is a wise strategy for human beings to replace traditional fossil energies with renewable energy. Solar cell is such a powerful device to perform the conversion of solar energy into electricity. P-type dye-sensitized solar cells (p-DSCs) have been developed rapidly during past decades. In this kind of solar cell, liquid redox couple electrolytes usually are used to undertake the electron transfer between photocathode and counter electrode. However, organic solvent is not a wise choice due to its volatile, flammable and hazardous properties. Moreover, in order to increase the achievable open circuit photovoltage (V_{OC}), the redox couple with negative

reduction potential is required; those redox couples featuring with the property always show poor stability under oxygen-included condition. In order to abandon the liquid phase and obtain an ideal V_{OC} in p-DSCs under moderate condition, the solid state p-type dye sensitized solar cells using electron conductor instead of liquid redox couple electrolyte is proposed for the first time. This work shows a new concept, experiment and mechanism of a new type of solar cell, aiming to realize real "stand-alone" p-DSCs.

Introduction

P-type dye sensitized solar cells (p-DSCs)[1] have attracted intense interest from scientists due to its potential application in tandem solar cells[2-4] and hydrogen generation devices[5-7]. In this kind of solar cell, a p-type semiconductor, such as NiO[1], Cu_2O[8], $CuCrO_2$[9] and $CuGaO_2$[10] sensitized by organic[3, 4, 11-14] or inorganic photosensitizers[14-22] is used as photocathode. In the typical p-DSC, a liquid electrolyte containing a redox couple is employed to undertake the internal electron transfer between photocathode and counter electrode. Iodide/triodide (I^-/I_3^-) was initially used as the redox couple in NiO-based p-DSC [1]; however, the open circuit voltage generated (V_{OC} <150 mV)[11, 12] is unsatisfying due to the small energy difference between the valence band edge (VB) of NiO (0.5 V vs. normal hydrogen electrode (NHE)) and the redox potential of I^-/I_3^- ($E^0 = 0.33$ V vs. NHE) [23]. In order to improve the V_{OC} of p-DSCs, increasing ΔE by using a redox couple with a more negative potential than I^-/I_3^- is desirable strategy. Gibson *et al.* used tris(ditert-butylbipyridine)cobalt(II/III) to obtain a V_{OC}=0.35 V.[2] Bach and co-workers reported two redox couples, tris(1,2-diaminoethane)cobalt(III)/(II)[24] and tris(acetylacetonato)iron(III)/(II)[25] with E^0 of -0.02 V and -0.2 V vs. NHE, respectively, in liquid p-DSC and obtained the V_{OC} more than 600 mV. However, redox couples with too negative potential are quite sensitive to oxygen and thus the solar cell fabrication has to be carefully carried out under O_2-excluding conditions, making the fabrication process more complicated; moreover, like most of liquid solar cells, the electrolyte leaking problem is still a drawback in the liquid p-DSCs. In order to completely abandon the liquid phase and still achieve a satisfactory V_{OC} in a p-DSC, in this paper, we propose and also prove the concept of solid state p-DSCs (p-ssDSCs), in which NiO is employed as the p-type semiconductor, an organic dye P1 as photosensitizer harvesting photons and an air-stable solid electron conductor, phenyl-C61-butyric acid methyl ester (PCBM), instead of liquid redox couple electrolyte, is employed as solid electron transfer material. Photovoltaic properties and time-resolved transient absorption spectroscopy are introduced to get insight into the mechanism of the proposed p-ssDSC model.

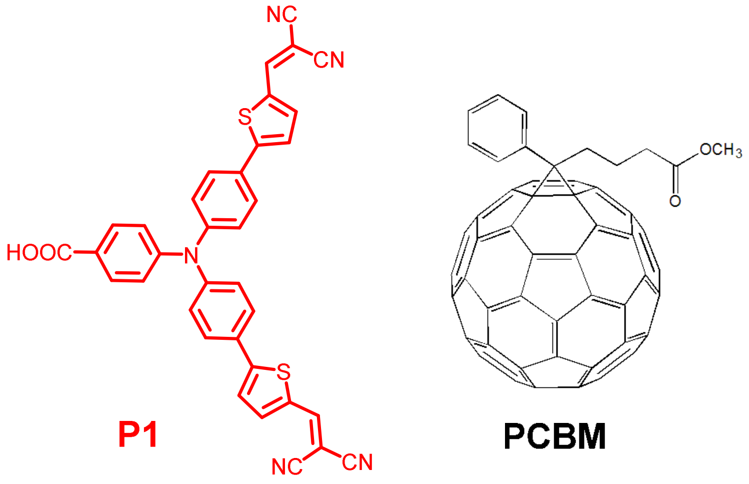

Figure 1. Structures of the compounds P1 and PCBM used in this study.

Results and discussion

Figure 1 depicts the structures of the compounds used in p-ssDSCs. P1 dye has a strong absorption in visible region and has been used as photosensitizer in liquid p-type DSCs before[11]. The previous publications have shown P1 is good photosensitizer for NiO sensitization and perform the effective hole injection in valence band (VB) of NiO,[11, 26] which encourages us to adopt it in this study.

Figure 2a shows the schematic drawing of p-ssDSCs, which consists of a 200 nm compact NiO layer (CL-NiO), a 700 nm mesoporous NiO layer (NL-NiO) sensitized by P1 as photocathode, a PCBM layer electron conductor and 100 nm Al counter electrode. Figure 2b gives the potential diagram of p-DSCs with different components. The potentials of all components vs. Normal Hydrogen Electrode (NHE) are adopted/converted from the literatures.[15, 26, 27] The compact NiO layer plays an important role to suppress the recombination process between the concentrated holes in FTO and reduced PCBM radical ($PCBM^{\bullet-}$). No photovoltaic performance is obtained from the device without a compact layer. According to the potential diagram (Figure 2b) of p-DSCs based on PCBM or I^-/I_3^-, one can see that the theoretical V_{OC} from p-ssDSC based on PCBM is determined to be 900 mV (from $E_{VB} - E^0_{PCBM/PCBM\bullet-}$), which is much higher than that from a liquid device using I^-/I_3^- as redox couple of only 200 mV. The driving force of electron transfer from the reduced state of $P1/P1^{\bullet-}$ to $PCBM/PCBM^{\bullet-}$ is 400 mV, implying that the process is thermodynamically feasible.

UV-vis absorption spectra of NiO films sensitized/coated with different components are shown in Figure 3. The P1 sensitized NiO film (NiO-P1) has a maximum absorption at 500 nm; however, when coated with PCBM afterwards, the sample NiO-P1/PCBM exhibits a superimposed absorption spectrum of P1 and PCBM absorption, in which the weak absorption at 710 nm is assigned to the characteristic absorption from PCBM (see NiO/PCBM sample). The photocurrent density-photovoltage (J-V) curves of devices measured under 100 $mW.cm^{-2}$ simulated sunlight illumination are presented in Figure 3a and the corresponding incident photon-to-electron conversion efficiency (IPCE) spectra are displayed in Figure 3b. The solar cell NiO-P1 without PCBM has no photovoltaic output and thus is not shown in these figures.

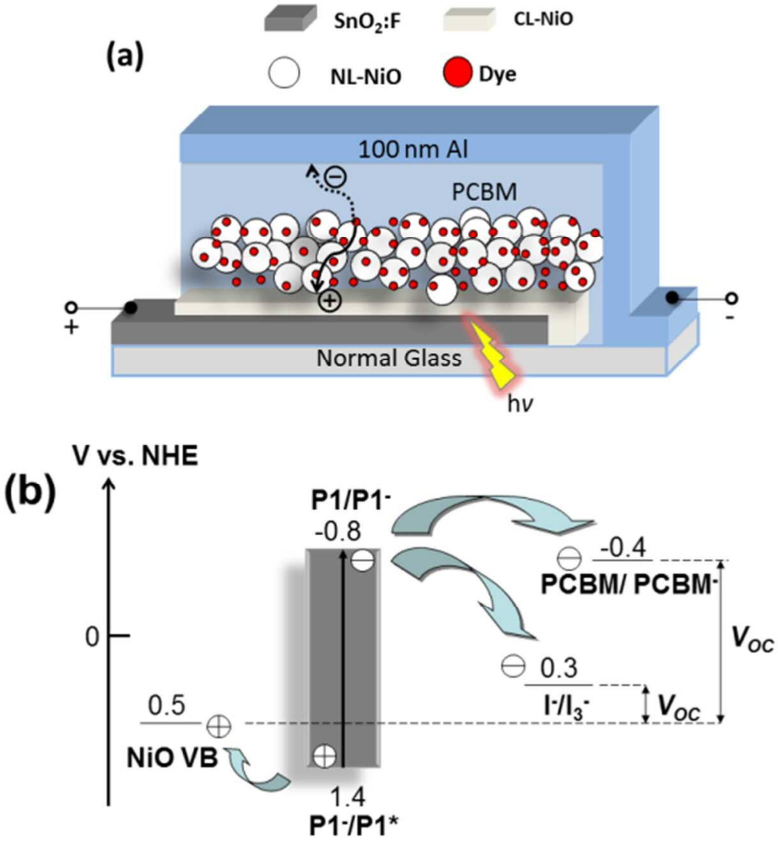

Figure 2. Schematic drawing of p-ssDSCs configuration (a) and potential diagram of p-DSCs based on PCBM or I^-/I_3^- (b).

As shown in Figure 4a, the device of NiO/PCBM shows a short-circuit photocurrent density (*Jsc*) of 11 $\mu A \cdot cm^{-2}$ and V_{OC} of 400 mV, indicating that electron/hole separation between PCBM and NiO takes place under light illumination. The E_{0-0} transition energy of PCBM can be estimated to be 1.8 eV by the absorption spectrum on NiO film. Therefore, the potential of $PCBM^*/PCBM^{\bullet -}$ is determined to be 1.4 V vs. NHE, which is more positive than VB potential of NiO, 0.5 V vs. NHE, implying that the hole injection from PCBM* is also thermodynamically feasible. After hole/electron separation at the interface of NiO and PCBM, the electrons in

PCBM will diffuse via PCBM layer to the counter electrode, thus producing certain photocurrent. With P1 as photosensitizer, the p-ssDSC device, NiO-P1/PCBM, rendered a *Jsc* of up to 50 $\mu A \cdot cm^{-2}$ and a V_{OC} of 620 mV, which are significantly improved in comparison to those generated from the NiO/PCBM device. From IPCE spectra (Figure 4b), the IPCE value of NiO-P1/PCBM is much higher than that of NiO/PCBM. The IPCE value of NiO-P1/PCBM in the region of P1 absorption (450-500 nm) is increased as compared to that of NiO/PCBM, which can be attributed to the charges generated from P1 absorption. Also, one can see that the IPCE around 710 nm is enhanced in the NiO-P1/PCBM device, which means that the hole injection efficiency from excited PCBM is also increased, probably due to the blocking effect of the P1 layer between NiO and PCBM to suppress the hole/electron recombination between NiO^+ and $PCBM^{\bullet -}$. Overall, the experiments suggest that P1 dye plays important role(s) in NiO-P1/PCBM device to improve the photovoltaic performance: acting as photosensitizer and/or blocking layer. In order to get insight into the mechanism of hole injection/electrons transfer in the device, femtosecond transient absorption spectroscopy measurements are carried out.

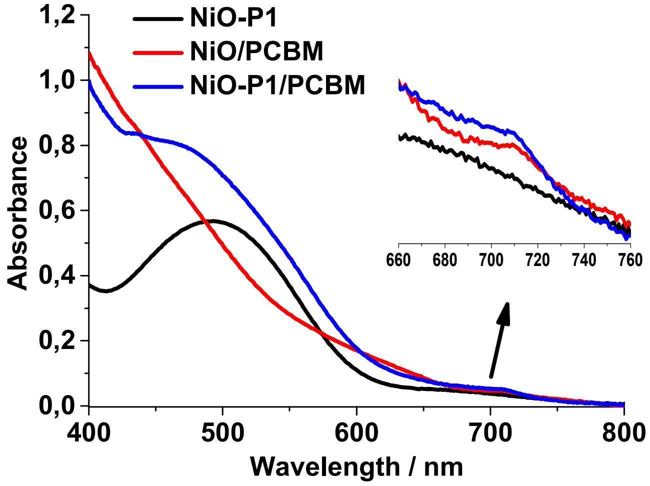

Figure 3. The UV-vis absorption of different components on NiO films (200 nm CL-NiO+700 nm NP-NiO).

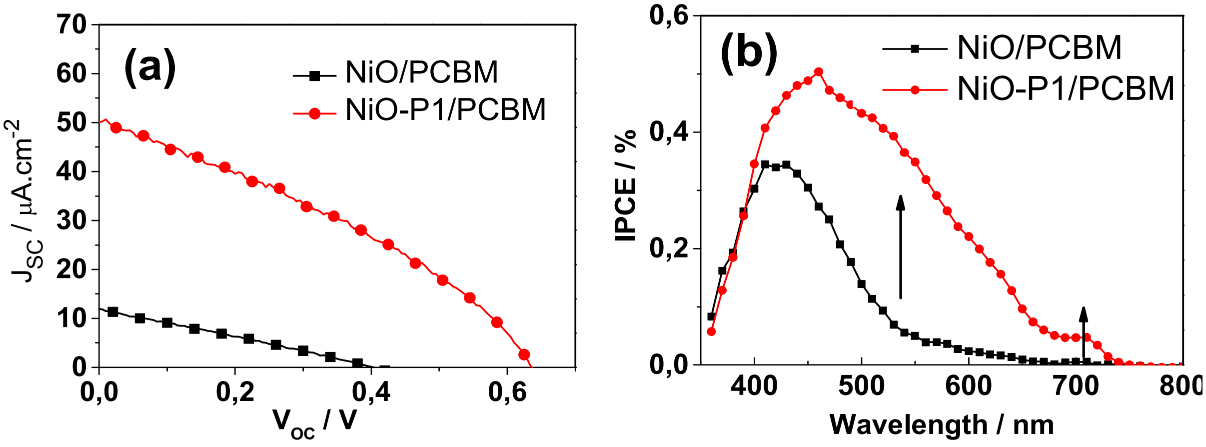

Figure 4. J-V curves (a) and IPCE spectra (b) of NiO/PCBM and NiO-P1/PCBM devices.

Both for NiO-P1 and NiO-P1/PCBM the fs transient absorption spectra after excitation at 525 nm (Figure 5a-b) give positive absorbance at ~420 nm and ~610 nm, and the P1 ground state bleach at ~500 nm. Already the spectrum at 0.3 ps can be described by a mix of the initial singlet excited P1 (^{1*}P1) and of the P1$^{\bullet-}$ formed by photoinduced hole injection. Some stimulated emission from ^{1*}P1 is apparent around 660 nm, but is gone already after a few ps. The strong 420 nm and 610 nm peaks are instead characteristic of P1$^{\bullet-}$[26] whereas ^{1*}P1 in solution shows a band around 550-560 nm and only weak transient absorption around 420 nm (Figure S1). Figure 6 shows transient absorption traces at 420 nm, monitoring the ultrafast formation of P1$^{\bullet-}$ by hole injection from the ^{1*}P1 to NiO. Ultrafast hole injection occurs with a time constant of ~200 fs, with slower injection components around 1-20 ps, all leading to formation of the charge separation state NiO^{+}/P1$^{\bullet-}$ (Figure 5a). This data is in agreement with the data in ref.26. During the slow hole injection phase, the absorption bands and isosbestic points shift further to the red. The signals also start to decrease due to charge recombination, which is multiphasic but has short ps components (see below).

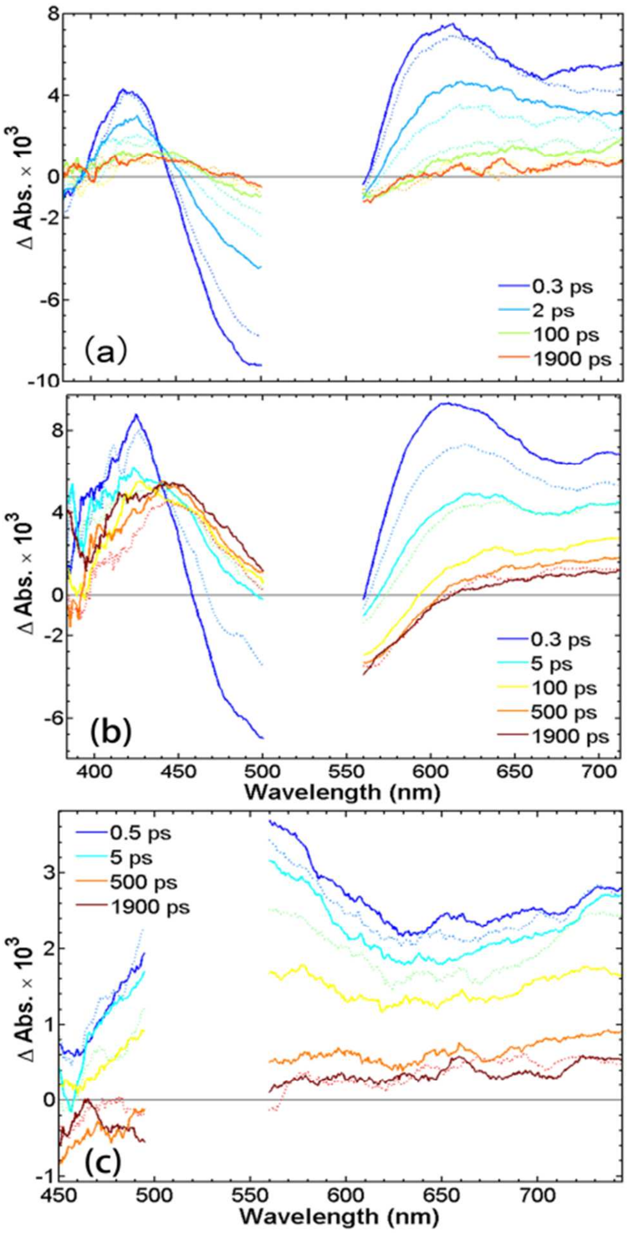

Figure 5. Transient absorption spectra for NiO-P1 (a), NiO-P1/PCBM (b) and NiO/PCBM (c) dry films (λ_{ex} = 525 nm, fwhm ~100 fs, 500 nJ/pulse; the solid lines are spectra at the given time delays after excitation, the dotted lines show spectra at intermediate times).

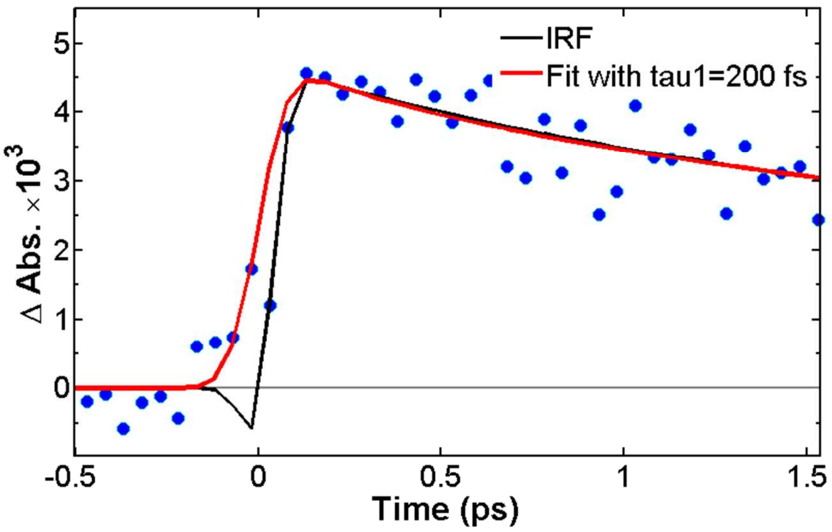

Figure 6. Transient absorption traces probed at 420 nm for NiO-P1, solid line is multi-exponential fit for each kinetic trace and black solid line shows IRF.

Also for the NiO-P1/PCBM transient spectrum (Figure 5b), the formation of P1$^{\bullet-}$ can be clearly observed. The main difference between NiO-P1 and NiO-P1/PCBM samples is at time scales > 5 ps when the signal for the latter around 450 nm is much larger. Importantly, while NiO-P1 shows an isosbestic point at 480 nm at long time scales, NiO-P1/PCBM shows a positive signal at the same wavelength that cannot be explained by formation of P1$^{\bullet-}$. Our control experiments show that the increased absorption at 450-500 nm for NiO-P1/PCBM also cannot be explained by absorption of PCBM$^{\bullet-}$, or formation of the P1 triplet excited state or P1$^{\bullet+}$ (due to electron transfer to PCBM, or bimolecular P1$^{\bullet+}$/P1$^{\bullet-}$ charge separation). This is because all these species show a net bleach in this spectral region (cf. Figure 5c, Figure S1 and Figures S3-S4, respectively). Finally, the triplet excited PCBM would have shown a prominent band around 670 nm [28] that is not seen in our data. After excluding these alternative, we instead attribute the transient spectra for NiO-P1/PCBM at t > 10 ps to a Stark effect shifting the ground state spectrum of the P1 molecules, due to the electric field of the NiO$^+$-P1/PCBM$^{\bullet-}$ state. Similar effects have been shown to be important for dye-sensitized TiO$_2$ systems.[29-31] In Figure S7 we show the first derivative of the absorption spectrum of P1, which is in good agreement with the transient spectra observed. Thus, our data suggest formation of the NiO$^+$-P1/PCBM$^{\bullet-}$ state on a time scale of 10s of ps, by electron transfer from NiO$^+$-P1$^{\bullet-}$/PCBM. A Stark effect could be contributing also to the transient spectra of NiO-P1, but the electric field effect of P1$^{\bullet-}$ on the neighboring P1 ground state molecules appears to be smaller (cf. Figures 5a-b).

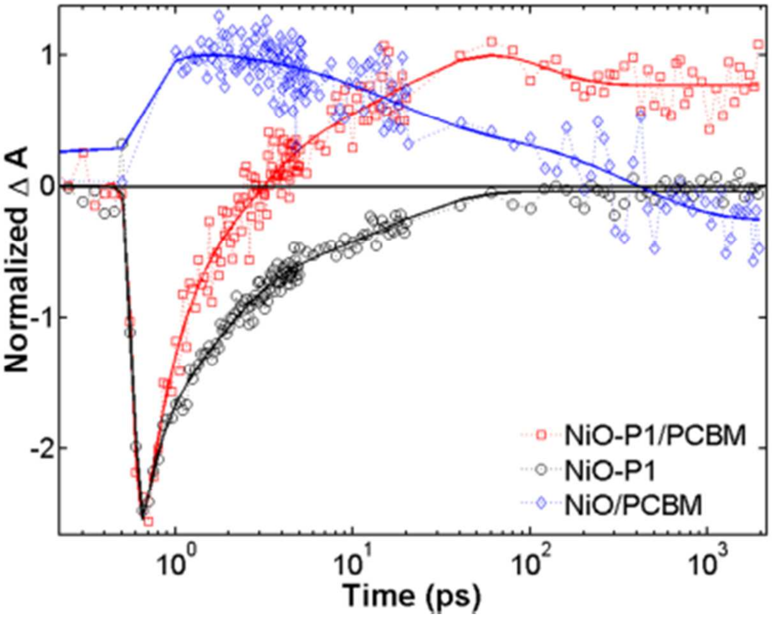

Figure 7. Comparison kinetics traces of all three systems probed at 480 nm, blue diamond is NiO/PCBM, red square is NiO-P1/PCBM and black cycle is NiO-P1, solid line is multi-exponential fit for each kinetic trace.

For comparison, P1/PCBM films cast on glass show initial features of the singlet excited states of both P1 and PCBM, which is about 40 ps form a spectrum we attribute to the P1$^{\bullet+}$/PCBM$^{\bullet-}$

charge separated state (see Figures S3-S4). The charge separation time scale in these films is much slower than for hole injection in NiO-P1 above, so that this alternative charge separation pathway should be negligible for P1 excitation in NiO-P1/PCBM, but may be important for the fraction of PCBM directly excited by light.

In the fs transient absorption spectra of NiO/PCBM shown in Figure 5c, a positive ~550 nm absorption appeared after excitation at 525 nm that can be assigned to the singlet state of fullerene, in agreement with the signal from pure PCBM on glass (Figure S2) as well as the data in literature[32]. The singlet PCBM should have a lifetime around 50 ns in absence of a quencher [32]. However, in the NiO/PCBM sample, the positive excited state signal around 500-550 nm has vanished in about 500 ps (Figure 5c) and instead a negative signal due to PCBM ground state bleach is obvious around 500 nm, indicating $NiO^+/PCBM^{\bullet -}$ formation after hole injection from the singlet excited state of PCBM to NiO. The $NiO^+/PCBM^{\bullet -}$ shows a very slow recombination process on the ns scale, as seen from the remaining transient absorption and the 700 nm ground state bleach from PCBM in ns experiments (Figure S2).

The fitting results with a sum of four exponentials were applied to the data in Figure 5 (see Table S2 for a summary of the data). Multi-exponential hole injection and recombination is typical for dye/NiO systems.[33] It is important to realize that a multi-exponential fit to data for a system with heterogeneous kinetics is an approximation to illustrate the time scales of a process rather than giving precise numbers. With that caveat in mind, the formation and decay of charge separation is illustrated by the kinetic traces at 480 nm (see Figure 7) where large qualitative differences between the samples are obvious. For NiO/PCBM, the initial signal of the PCBM singlet excited state is positive, and a 300 fs component is assigned to vibrational relaxation. Then the spectrum decays with little change of shape, with 15 ps and ≈400 ps time constants, to result in net bleach around 480 nm, which is attributed to hole injection into NiO. For NiO-P1, the initial signal at 480 nm is mainly a P1 ground state bleach. The bleach recovery follows two ultrafast components with time constants of ~200 fs (38%) and 1.3 ps (39%). These are attributed to hole injection, based on the shift in absorption peaks and stimulated emission discussed above. The slower time constants (20 ps and ∞) are attributed to charge recombination between the hole and the reduced dye.

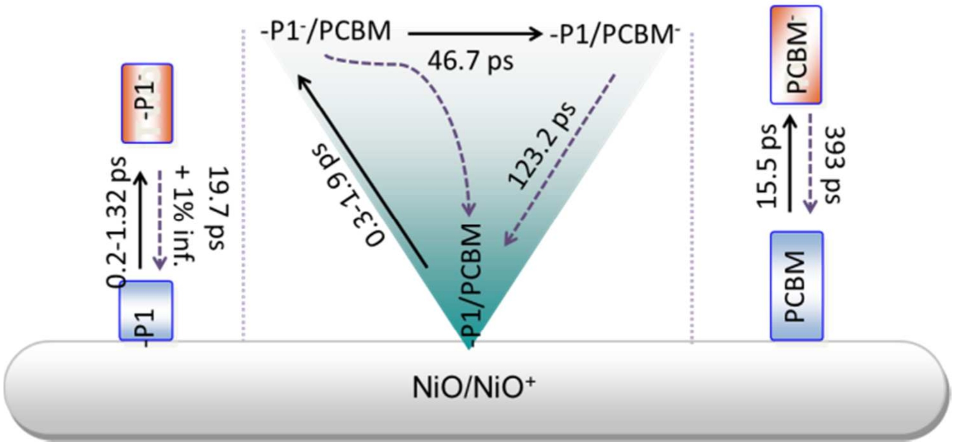

Figure 8. General charge transfer scheme with approximate time constants for each system. Solid arrows denote positive process (hole injection and electron transfer), dashed arrows present recombination processes.

When PCBM was employed as electron conductor on the NiO-P1 in NiO-P1/PCBM, the bleach recovery follows essentially the same time constants as without PCBM, of about 300 fs (34%) and 1.9 ps (18%) (see Figure S6). However, the magnitude of bleach recovery is greater, and during a 47 ps component a positive absorption grows in. This results in the Stark shifted ground state spectrum. By inspecting the wavelength shift of the 420 nm band and the 450-500 nm isosbestic point (Figure 5b), we conclude that the faster two components mainly form NiO^{+}-P1$^{\bullet -}$ and that most of the charge shift to form NiO-P1/PCBM$^{\bullet -}$ is represented by the 47 ps component (see Figure 8). After that, a small decay component is observed with ca. 120 ps time constant, which is similar to that observed for NiO-PCBM. This indicates partial recombination, but most of the signal remains at 0.1-2 ns, indicating a long-lived charge separation due to the PCBM acceptor layer. The fraction of direct PCBM excitation is small compared to that of P1 and cannot be directly seen in the transient absorption data. The enhanced IPCE around 710 nm due PCBM is, however, clear evidence for additional charge separation generated from PCBM excitation that leads to photocurrent generation. We cannot determine if this fraction reacts by direct hole injection or via initial formation of $P1^{\bullet+}/PCBM^{\bullet-}$.

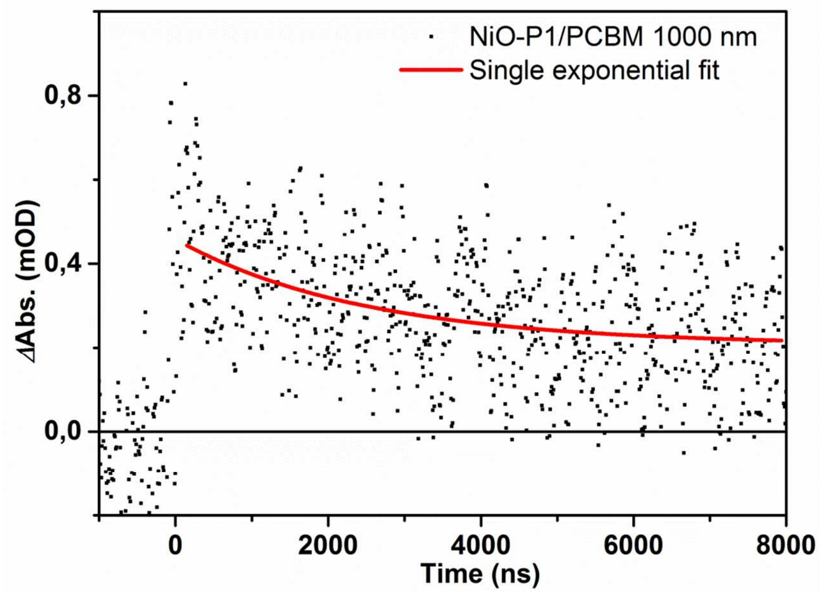

Figure 9. NIR kinetics traces of NiO-P1/PCBM at 1000 nm with excitation at 532 nm (10 mJ/pulse).

In order to further detect $PCBM^{\bullet-}$ in the samples, all samples were excited with a 10 ns flash and probed around 1000 nm with, where $PCBM^{\bullet-}$ shows a characteristic absorption maximum[34-36]. From Figure 9, a clear instrument-limited absorption rise followed by a decay on the microsecond time scale can be observed in NiO-P1/PCBM sample. The kinetics traces of

NiO/PCBM and P1/PCBM on glass are presented in the Figure S6, P1/PCBM on glass shows the strongest signal at 950 nm, which is evidence to show $PCBM^{\bullet-}$ formed by electron transfer from excited P1 dye. NiO/PCBM presents no clear signal, implying that the amount of $PCBM^{\bullet-}$ generated by directed hole injection from PCBM* to VB of NiO, and still remaining on the time scale of >10 ns, is much smaller than that from the NiO-P1/PCBM sample. This is probably the main reason that the NiO-P1/PCBM device has better photovoltaic performance than the NiO/PCBM device.

In a summary of ultrafast transient absorption results, we have shown that all samples on NiO give rapid hole injection, for P1 this occurs to a large extent on the 200-300 fs time scale, followed by ps components. For NiO-P1/PCBM the reduced $P1^{\bullet-}$ transfers an electron to the added PCBM acceptor layer, predominantly in a 47 ps component, to form the long-lived (>>1 ns) NiO^{+}-P1/$PCBM^{\bullet-}$. The 47 ps time scale is similar to that of charge recombination in the absence of PCBM, which suggests that recombination of NiO^{+}-$P1^{\bullet-}$/PCBM competes with charge shift to PCBM and therefore is one limitation to the device efficiency. NIR transient absorption experiments show that the $PCBM^{\bullet-}$ is generated after light illumination, and that a higher concentration remains after > 8 μs in the NiO-P1/PCBM sample than the NiO/PCBM sample.

Conclusion

In conclusion, we proposed the solid state p-type dye sensitized solar cells (p-ssDSCs) for the first time. The photovoltaic data have shown the feasibility of this concept. Ultrafast transient absorption spectroscopy was employed to successfully investigate the electron transfer processes in this system. An electron transfer from $P1^{\bullet-}$ formed after hole injection to NiO and electron transfer from $P1^{\bullet-}$ to the electron conductor PCBM can be dynamically feasible. The low efficiency of the device shown in this work could be due to the unsatisfactory lifetime of $P1^{\bullet -}$ or slow dye regeneration from PCBM. The future work will focus on optimizing and improving the efficiency by seeking a dye/material with long lived charge separation state or a new electron transport material with highly efficient dye regeneration ability. The development of highly efficient p-ssDSCs will also pave the way to construct all solid state tandem dye sensitized solar cells.

Supporting Information.

The details of solar cell fabrication and measurements; ultrafast transient absorption of P1 in solution, other transient absorption spectra of different control experiments, DAS spectra, NIR kinetics traces of different samples, etc. This material is available free of charge via the Internet at http://pubs.rsc.org

Acknowledgement

The authors acknowledge the foundation support from the Knut & Alice Wallenberg Foundation and the Swedish Energy Agency. We would like to greatly thank Bo Xu, Dr. Erik Gabrielsson, Prof. Lars Kloo and Prof Licheng Sun at KTH, and Dr. Zaifei Ma and Prof. Fengling Zhang at Linköpings University (LiU) for their helpful discussion. We also would like to acknowledge Jens Föhlinger, Dr. Abhinandan Makhal, Dr. Jonas Petersson at UU for kindness help. L. Z. also thanks China Scholarship Council (CSC) for the scholarship support.

References

1. J. He, H. Lindström, A. Hagfeldt and S.-E. Lindquist, *J. Phys. Chem. B*, 1999, **103**, 8940-8943.
2. E. A. Gibson, A. L. Smeigh, L. Le Pleux, J. Fortage, G. Boschloo, E. Blart, Y. Pellegrin, F. Odobel, A. Hagfeldt and L. Hammarström, *Angew. Chem. Int. Ed.*, 2009, **48**, 4402-4405.
3. A. Nattestad, A. J. Mozer, M. K. R. Fischer, Y. B. Cheng, A. Mishra, P. Bauerle and U. Bach, *Nat Mater*, 2010, **9**, 31-35.

4. C. J. Wood, G. H. Summers and E. A. Gibson, *Chem. Commun.*, 2015, **51**, 3915-3918.
5. L. Li, L. Duan, F. Wen, C. Li, M. Wang, A. Hagfeldt and L. Sun, *Chem. Commun.*, 2012, **48**, 988-990.
6. Z. Ji, M. He, Z. Huang, U. Ozkan and Y. Wu, *J. Am. Chem. Soc.*, 2013, **135**, 11696-11699.
7. L. Tong, A. Iwase, A. Nattestad, U. Bach, M. Weidelener, G. Gotz, A. Mishra, P. Bauerle, R. Amal, G. G. Wallace and A. J. Mozer, *Energy Environ. Sci.*, 2012, **5**, 9472-9475.
8. S. Du, P. Cheng, P. Sun, B. Wang, Y. Cai, F. Liu, J. Zheng and G. Lu, *Chem. Res. Chin. Univ.*, 2014, **30**, 661-665.
9. S. Powar, D. Xiong, T. Daeneke, M. T. Ma, A. Gupta, G. Lee, S. Makuta, Y. Tachibana, W. Chen, L. Spiccia, Y.-B. Cheng, G. Götz, P. Bäuerle and U. Bach, *J. Phys. Chem. C*, 2014, **118**, 16375-16379.
10. M. Yu, T. I. Draskovic and Y. Wu, *Phys. Chem. Chem. Phys.*, 2014, **16**, 5026-5033.
11. P. Qin, H. Zhu, T. Edvinsson, G. Boschloo, A. Hagfeldt and L. Sun, *J. Am. Chem. Soc.*, 2008, **130**, 8570-8571.
12. P. Qin, M. Linder, T. Brinck, G. Boschloo, A. Hagfeldt and L. Sun, *Adv. Mater.*, 2009, **21**, 2993-2996.
13. L. Favereau, J. Warnan, Y. Pellegrin, E. Blart, M. Boujtita, D. Jacquemin and F. Odobel, *Chem. Commun.*, 2013, **49**, 8018-8020.
14. M. Gennari, F. Légalité, L. Zhang, Y. Pellegrin, E. Blart, J. Fortage, A. M. Brown, A. Deronzier, M.-N. Collomb, M. Boujtita, D. Jacquemin, L. Hammarström and F. Odobel, *J. Phys. Chem. Lett.*, 2014, **5**, 2254-2258.
15. H. Tian, J. Oscarsson, E. Gabrielsson, S. K. Eriksson, R. Lindblad, B. Xu, Y. Hao, G. Boschloo, E. M. J. Johansson, J. M. Gardner, A. Hagfeldt, H. Rensmo and L. Sun, *Sci. Rep.*, 2014, **4**, 4282.
16. F. Safari-Alamuti, J. R. Jennings, M. A. Hossain, L. Y. L. Yung and Q. Wang, *Phys. Chem. Chem. Phys.*, 2013, **15**, 4767-4774.
17. H. Tian, B. Xu, H. Chen, E. M. Johansson and G. Boschloo, *ChemSusChem*, 2014, **7**, 2150-2153.
18. Z. Ji, G. Natu and Y. Wu, *ACS Applied Materials & Interfaces*, 2013, **5**, 8641-8648.
19. Z. Ji, G. Natu, Z. Huang, O. Kokhan, X. Zhang and Y. Wu, *J. Phys. Chem. C*, 2012, **116**, 16854-16863.
20. C. J. Wood, K. C. D. Robson, P. I. P. Elliott, C. P. Berlinguette and E. A. Gibson, *RSC Advances*, 2014, **4**, 5782-5791.
21. K.-C. Wang, J.-Y. Jeng, P.-S. Shen, Y.-C. Chang, E. W.-G. Diau, C.-H. Tsai, T.-Y. Chao, H.-C. Hsu, P.-Y. Lin, P. Chen, T.-F. Guo and T.-C. Wen, *Sci. Rep.*, 2014, **4**.
22. Z. Zhu, Y. Bai, T. Zhang, Z. Liu, X. Long, Z. Wei, Z. Wang, L. Zhang, J. Wang, F. Yan and S. Yang, *Angew. Chem. Int. Ed.*, 2014, **53**, 12571-12575.
23. E. A. Gibson, A. L. Smeigh, L. Le Pleux, L. Hammarström, F. Odobel, G. Boschloo and A. Hagfeldt, *J. Phys. Chem. C*, 2011, **115**, 9772-9779.
24. S. Powar, T. Daeneke, M. T. Ma, D. Fu, N. W. Duffy, G. Götz, M. Weidelener, A. Mishra, P. Bäuerle, L. Spiccia and U. Bach, *Angew. Chem. Int. Ed.*, 2013, **52**, 602-605.
25. I. R. Perera, T. Daeneke, S. Makuta, Z. Yu, Y. Tachibana, A. Mishra, P. Bäuerle, C. A. Ohlin, U. Bach and L. Spiccia, *Angew. Chem. Int. Ed.*, 2015, **54**, 3758-3762.

26. P. Qin, J. Wiberg, E. A. Gibson, M. Linder, L. Li, T. Brinck, A. Hagfeldt, B. Albinsson and L. Sun, *J. Phys. Chem. C*, 2010, **114**, 4738-4748.
27. J. J. Benson-Smith, H. Ohkita, S. Cook, J. R. Durrant, D. D. C. Bradley and J. Nelson, *Dalton Trans.*, 2009, 10000-10005
28. D. M. Guldi and M. Prato, *Acc. Chem. Res.*, 2000, **33**, 695-703.
29. U. B. Cappel, S. M. Feldt, J. Schöneboom, A. Hagfeldt and G. Boschloo, *J. Am. Chem. Soc.*, 2010, **132**, 9096-9101.
30. S. Ardo, Y. Sun, A. Staniszewski, F. N. Castellano and G. J. Meyer, *J. Am. Chem. Soc.*, 2010, **132**, 6696-6709.
31. U. B. Cappel, A. L. Smeigh, S. Plogmaker, E. M. J. Johansson, H. Rensmo, L. Hammarström, A. Hagfeldt and G. Boschloo, *J. Phys. Chem. C*, 2011, **115**, 4345-4358.
32. D. M. Guldi and M. Prato, *Accounts Chem Res*, 2000, **33**, 695-703.
33. F. Odobel, Y. Pellegrin, E. A. Gibson, A. Hagfeldt, A. L. Smeigh and L. Hammarström, *Coord. Chem. Rev.*, 2012, **256**, 2414-2423.
34. H. Ohkita, S. Cook, Y. Astuti, W. Duffy, S. Tierney, W. Zhang, M. Heeney, I. McCulloch, J. Nelson, D. D. C. Bradley and J. R. Durrant, *J. Am. Chem. Soc.*, 2008, **130**, 3030-3042.
35. C. D. Weber, C. Bradley and M. C. Lonergan, *J. Mater. Chem. A*, 2014, **2**, 303-307.
36. J. Xu, A. Buin, A. H. Ip, W. Li, O. Voznyy, R. Comin, M. Yuan, S. Jeon, Z. Ning, J. J. McDowell, P. Kanjanaboos, J.-P. Sun, X. Lan, L. N. Quan, D. H. Kim, I. G. Hill, P. Maksymovych and E. H. Sargent, *Nat Commun*, 2015, **6**.